Ferromagnetic transition of $SrRuO_3$ in nanometer thick bilayers with $YBa_2Cu_3O_y$, $La_{1.88}Sr_{0.12}CuO_{4-y}$, Au, and Cr: Signature of injected carriers in the pseudogap regime

G. Aharonovich, G. Koren,* and E. Polturak
Physics Department, Technion-Israel Institute of Technology, Haifa 32000, Israel
(Received 17 May 2007; published 13 December 2007)

The hypothesis regarding the existence of uncorrelated preformed pairs in the pseudogap regime of superconducting $YBa_2Cu_3O_y$ is tested experimentally using bilayers of $YBa_2Cu_3O_y$ and the itinerant ferromagnet $SrRuO_3$. In our study, we monitor the influence of $YBa_2Cu_3O_y$ on T_p, the ferromagnetic ordering temperature of $SrRuO_3$. Here, T_p is the temperature of maximum dM/dT or dR/dT, where M and R are the magnetization and resistance of $SrRuO_3$, respectively. We compare the results with similar measurements carried out on bilayers of $La_{1.88}Sr_{0.12}CuO_{4-y}$, Au, and Cr with $SrRuO_3$. We find that in bilayers made of underdoped 10 nm $YBa_2Cu_3O_y$/5 nm $SrRuO_3$, the T_p values are shifted to lower temperatures by up to 6–8 K as compared to $T_p \approx 140$ K of the 5 nm thick reference $SrRuO_3$ film. In contrast, in the other type of bilayers, which are not in the pseudogap regime near T_p, only a smaller shift of up to ±2 K is observed. These differences are discussed in terms of a proximity effect, where carriers from the $YBa_2Cu_3O_y$ layer are injected into the $SrRuO_3$ layer and vice versa. We suggest that correlated electrons in the pseudogap regime of $YBa_2Cu_3O_y$ are responsible for the observed large T_p shifts.

DOI: 10.1103/PhysRevB.76.224514 PACS number(s): 74.45.+c, 75.70.−i, 74.50.+r, 74.78.Bz

There exists a large body of experimental evidence to date for the existence of a pseudogap regime above T_c in the high temperature superconducting cuprates.[1,2] Among the several possible models put forward to explain the origin of this phenomenon, the precursor pair scenario carries a certain appeal. This model assumes the existence of preformed pairs in the pseudogap regime which do not show phase coherence. On lowering the temperature, these precursor pairs reach phase coherence at the superconducting transition temperature T_c.[3] The preformed pair scenario is consistent with many experimental results in the pseudogap regime, but experimental verification for the existence of the elusive preformed pairs is still lacking. In the present study, we investigate the proximity effect in the pseudogap regime using bilayers of $YBa_2Cu_3O_y$ (YBCO) and the itinerant ferromagnet $SrRuO_3$ (SRO). We observe that the proximity effect leads to a large decrease of the ferromagnetic transition temperature. Ferromagnetic order is incompatible with singlet Cooper pairs. Consequently, the presumed preformed pairs are likely candidates to explain this effect. Previous results on the proximity effect using superconducting-ferromagnetic bilayers and multilayers have been reported mostly for YBCO and a manganite such as $La_{2/3}Ca_{1/3}MnO_3$ (LCMO) showing giant magnetoresistance. It was shown by magnetization measurements that the temperatures where the magnetic moment saturates below the superconducting T_c and of the onset of the ferromagnetic transition at T_{Curie} above T_c are both suppressed with increasing thickness of the superconducting layer.[4] The results above T_c were interpreted as due to a possible charge transfer from the LCMO to the YBCO layer. Similar results on the suppression of T_{Curie} versus the YBCO thickness in multilayers of YBCO/LCMO above T_c were obtained also in resistivity and susceptibility measurements.[5,6] The opposite effect where the superconducting T_c is depressed by the ferromagnetic layer is also possible due to pair breaking by spin polarized carriers penetrating the superconductor.[4,5,7] No reference to the pseudogap or preformed pairs role in this context was mentioned or discussed in these studies.

In our experiment, epitaxial thin films and bilayers of SRO with either YBCO, $La_{1.88}Sr_{0.12}CuO_{4-y}$ (LSCO), Cr, or Au were deposited *in situ* by laser ablation deposition on (100) $SrTiO_3$ (STO) wafers of 10×10 mm^2 area. For reference, nominally identical single layer films of these materials on STO were also prepared. All SRO, YBCO, and LSCO layers in the different heterostructures were oriented with their c axis normal to the wafer. The SRO and LSCO layers were prepared under the same deposition conditions as for obtaining high quality YBCO films (100 mT of oxygen flow and at 780 °C). The Cr layer was deposited under vacuum at 30 °C, while the Au layer was deposited in 400 mT oxygen at 150 °C. Transmission electron microscope (TEM) images of similar SRO films deposited on (100) STO show an atomically smooth interface with the STO wafer and were found to grow in the layer-by-layer mode up to at least 10 nm thickness.[8] Figure 1 shows an image of the surface morphology of one of our SRO films measured by a scanning tunneling microscope (STM). One can see that this film consists of a stack of parallel and flat plates which are ~60–90 nm wide and atomically smooth. These plates are separated by steps of one unit cell height (the c axis of SRO) and are formed due to the ~0.5° miscut angle of the STO substrate. Thus, the area onto which the cover layers in the bilayers with SRO are deposited on is atomically smooth and almost flat. In view of the small fraction of the total area of the film that the atomic steps occupy, we can safely assume that the dominant contribution to the properties of the bilayers originates in the flat areas. TEM images of the YBCO/SRO interface are also atomically smooth[9] and similar to the YBCO/LCMO interfaces in superlattices.[10] We can therefore conclude that the sharp and flat interfaces exclude any interdiffusion and chemical reactions which could affect our results. Recently, epitaxial $SrTiO_3/LaAlO_3$ bilayers with different termination layers at the interface were investigated.[11]

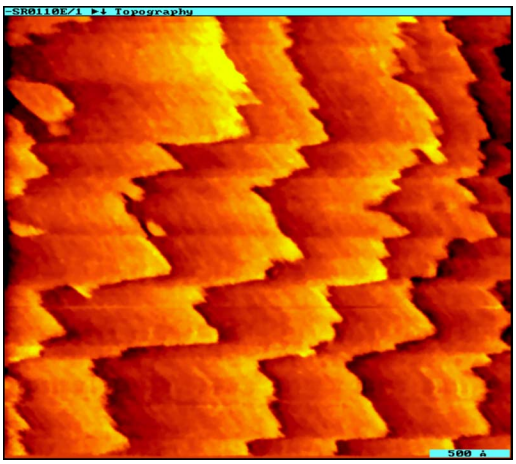

FIG. 1. (Color online) A scanning tunneling microscope image of 300×300 nm^2 area, showing the surface morphology of a typical SRO film deposited on (100) STO wafer. The observed plates are atomically smooth, and the steps between them are of one unit cell in height in the c direction of SRO (0.785 nm).

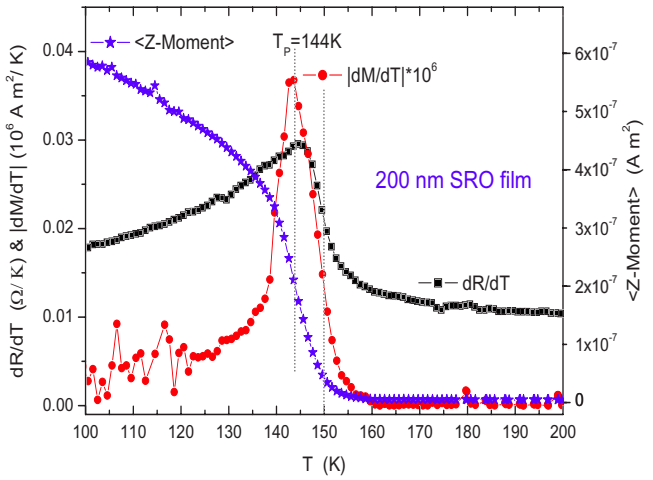

FIG. 2. (Color online) Temperature derivative of the resistance versus temperature of a 200 nm thick SRO film, together with the magnetization of the same film and its temperature derivative.

The results show that the effects of ionic and charge compensation for the different cases play a major role in enabling the creation of a sharp interface on a scale of a single atomic layer. In that study, however,[11] both components of the bilayer are ionic and insulating, while in our case, all the layers are metallic and conducting. Therefore, charge compensation is taken care of automatically, and the resulting interfaces are smooth and sharp. We also note that even if only one layer in the bilayer is conducting like in the SRO/STO case, the interface is clearly sharp.[8]

In order to minimize effects of wafer to wafer variations between different deposition runs, some bilayers were prepared *in situ* together with the reference films in the following way: First, the SRO layer was deposited on the whole area of the wafer. Then, a shadow mask made of a MgO wafer was used to cover half of the sample area while the YBCO layer was deposited on the other half. This resulted in an SRO reference film on half the wafer and a bilayer on the other half. The various single layer films and bilayers deposited on the whole area of the wafer were not patterned. Wafers which were half coated with a bilayer and half with the SRO film were patterned by either wet etching or a scratch of a narrow stripe to separate the bilayer from the reference film. A very convenient feature of our experiment was that YBCO/SRO bilayers could be reannealed in O_2 to produce YBCO with different values of T_c without affecting the properties of the SRO. We note that the oxygen annealing process was done at 450 °C, which is about half the deposition temperature, and was fully reversible. Namely, we could switch back and forth between the different T_c values of the bilayers without any change in their properties. This again is consistent with the absence of interdiffusion which would have affected the properties of the bilayer in a progressive and irreproducible manner. This convenient feature allowed us to compare the proximity effects at different doping levels on the same sample. Transport measurements were done by the standard four-probe technique using gold coated contact tips. All in all, about 30 bilayers and reference films were prepared and measured to establish the reliability and reproducibility of our results.

In the present study, resistance versus temperature measurements were used rather than direct magnetization measurements, because of the higher sensitivity that can be obtained in measuring a few nanometer thick SRO film (typically 5 nm). Theoretically, the issue of resistive anomalies and peaks associated with ferromagnetic transitions was discussed quite long ago.[12,13] Here, we wish to show first, experimentally, that near the ferromagnetic transition, the functional dependence of dR/dT is very similar to that of dM/dT, where R is the resistance, T is the temperature, and M is the magnetization of the sample. For this, magnetization measurements as a function of temperature were performed using a superconducting quantum interference device magnetometer and compared with measurements of R and dR/dT of the same sample. Figure 2 shows the results of these measurements on a 200 nm thick SRO film. One can see that on cooling down, the magnetization curve starts rising at $T_{Curie}\approx150$ K, where the ferromagnetic order sets in, and that this temperature coincides with the corresponding sharp increase of both dR/dT and dM/dT. The inflection point of M versus T yields a peak in dM/dT, which also coincides with the peak of dR/dT. We denote this temperature by T_p. Thus, a basic correspondence between dR/dT and dM/dT near T_{Curie} is well established. For the thin films of a few nanometer thickness used in this study, the magnetization signal was too small to measure. We therefore used measurements of dR/dT to detect T_p, the midpoint of the ferromagnetic transition.

The choice of thickness of the films in this study was done by searching for the combination that would produce a large observable effect on the SRO transition. In general, to achieve good sensitivity, the resistances of the two components of the bilayer should be comparable. Second, the thickness should be in the range of the relevant penetration depths of the proximity effect. If one of the layers is much thicker than the penetration depth, the observable effect will be small. For example, with the YBCO film much thicker than

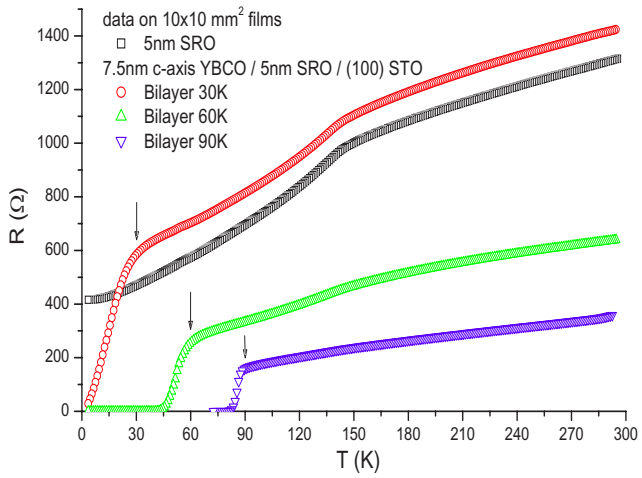

FIG. 3. (Color online) Resistance versus temperature of a 5 nm SRO film and of a 7.5 nm YBCO/5 nm SRO bilayer reannealed under different conditions to produce YBCO with T_c of either 90, 60, or 30 K (see the arrows).

the SRO, the SRO transition was suppressed to the point where an unambiguous identification of T_p became impossible. Finally, if the layers are too thin, the number of carriers available for injection into the other film is too small to produce an observable effect. For example, as shown below, in bilayers of 7.5 nm YBCO on 5 nm SRO, any suppression of the SRO transition temperature was smaller than the variation of T_p between different SRO films. In contrast, a clear suppression was observed in bilayers of 10 nm YBCO on 5 nm SRO. The thickness of the films used in this study indicates that the range of the proximity effect is on the order of a few nanometers. In view of the effects discussed above concerning the layers thickness in the bilayers, we also conclude that the measured results in the bilayers reflect mostly their bulk properties and not the interface.

Figures 3 and 4 show the resistance versus temperature and the corresponding temperature derivatives dR/dT of a

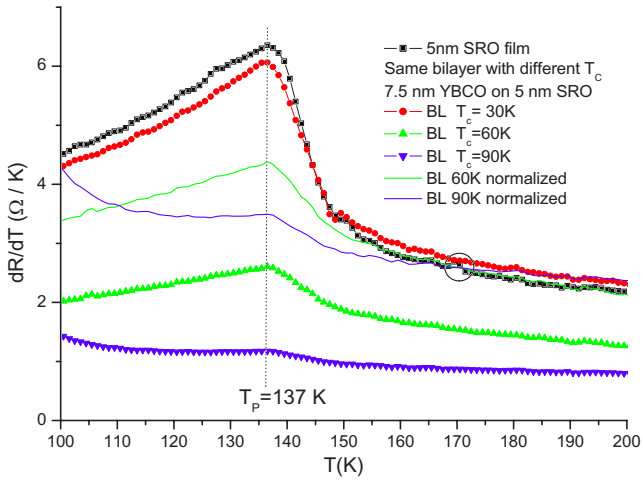

FIG. 4. (Color online) Temperature derivatives dR/dT of the resistance versus temperature data of Fig. 3. The curves without symbols represent the 60 and 90 K bilayer data normalized to the reference SRO data in the temperature range indicated by the circle.

5 nm thick SRO film and of a 7.5 nm YBCO/5 nm SRO bilayer under three different oxygenation levels. The value of T_p in 5 nm thick SRO films is typically around 137–140 K, slightly lower than in the bulk (144 K, as seen in Fig. 2). It was established independently that the SRO films are insensitive to the oxygen annealing conditions used in the present study. In contrast, the YBCO layer in the bilayer is very sensitive to the oxygen annealing conditions, and in Figs. 3 and 4, we show the results for the 30, 60, and 90 K phases of YBCO obtained on the same bilayer through repeated annealing. We note that the oxygen annealing process is reversible, as we can switch between different T_c values with reproducible transport results. This multiple annealing without deterioration in the transport properties is apparently due to the fact that the oxygen annealing temperature (450 °C) is much lower than the deposition temperature (780 °C) where the layered structure is formed. Figure 4 shows that at temperatures above 100 K, the 30 K bilayer data are almost coincident with that of the SRO film. This is due to the high normal resistivity of the 30 K YBCO phase and indicates very little interaction between the layers in this case. For the 60 and 90 K phases of YBCO, this is no longer the case. A suppression of the magnitude of dR/dT near T_p is clearly observed. To account for the different resistances of the differently oxygenated bilayers as in Fig. 3, and for the sample to sample variability due to morphology differences and so on, we generally normalized the dR/dT data to that of the SRO reference film in the temperature range of 160–180 K above the ferromagnetic transition at T_{Curie}=150 K. In cases where the dR/dT curves did not fully overlap in this regime, normalization was done around 170 K, such as in Fig. 4. The normalized curves show that T_p, the midpoint of the ferromagnetic transition (shown by the curves without symbols in Fig. 4), remains constant at 137 K, but the overall magnitude of the dR/dT signal is still significantly suppressed in these bilayers.

In the next step, we prepared bilayers with a slightly thicker YBCO layer. Figure 5 shows the dR/dT data versus temperature of a bilayer of 10 nm thick YBCO film on top of a 5 nm thick SRO layer, together with the data of the corresponding reference films. Also shown in Fig. 5 is the expected resistance of the same bilayer structure, calculated when the two layers are assumed to be noninteracting and behave like two independent resistors connected in parallel (termed "calculated" in Fig. 5). The bilayer and films were annealed in a low oxygen pressure (of 10 mTorr O_2 flow) to produce the T_c=60 K phase of YBCO. At this doping level, the pseudogap regime of YBCO sets in below T^* of about 170–200 K (this is seen as the broad shallow peak of the YBCO film in Fig. 5). As before, the SRO films are found to be insensitive to the oxygen annealing pressure, with T_{Curie} of 150 K. This is easily seen by the change of slope at 150 K of the resistance versus temperature curve of the SRO film in Fig. 3 and by the corresponding sharp increase of dR/dT in Fig. 5 at 150 K. These observations are in agreement with the results found in the literature.[14,15] Just below 150 K, the measured dR/dT of the bilayer in Fig. 5 is clearly lower than the calculated resistance of the corresponding noninteracting bilayer. Thus, one can conclude that the different layers do affect one another in such a way that decreases their dR/dT

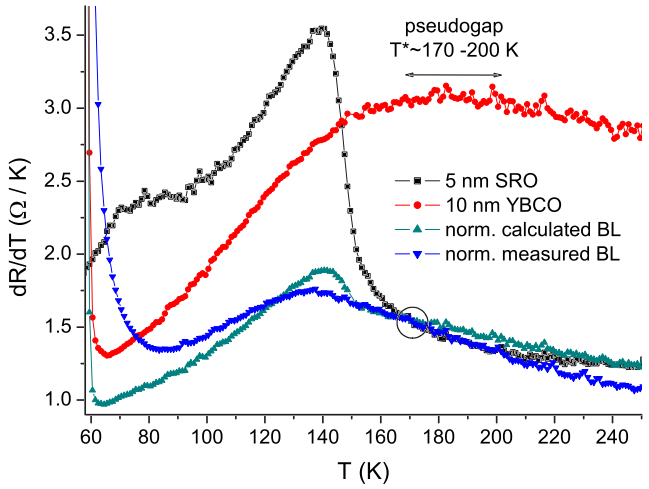

FIG. 5. (Color online) Temperature derivatives dR/dT of the resistance versus temperature of a 5 nm thick SRO film and a 10 nm thick 60 K YBCO film together with the normalized data of the measured and calculated results of 10 nm YBCO/5 nm SRO bilayers. The bilayer curves are normalized to the reference SRO data at 170 K as indicated by the circle.

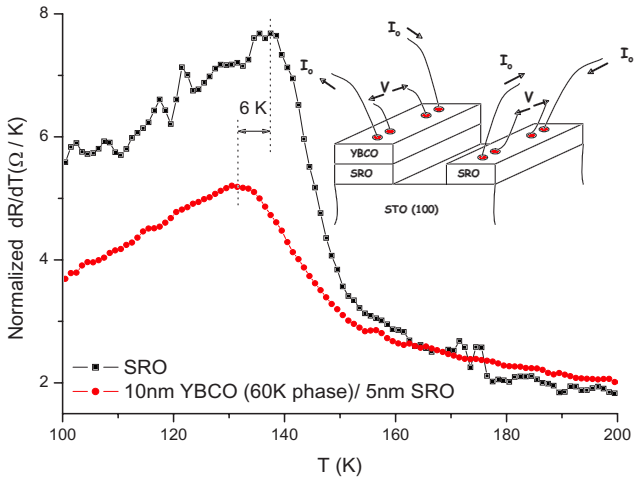

FIG. 7. (Color online) dR/dT versus temperature of a 10 nm YBCO (60 K phase)/5 nm SRO bilayer normalized to its 5 nm thick SRO reference film on the same wafer. Normalization is done in the 160–180 K temperature range. The inset shows a schematic drawing of the bilayer and reference film on the wafer together with the two four-probe contact configuration.

below the ferromagnetic transition temperature. Here, a shift of the ferromagnetic peak temperature T_p to lower temperatures is observed, and this will be discussed in more detail next.

Figure 6 shows dR/dT results versus temperature of a 10 nm YBCO/5 nm SRO bilayer obtained on the same wafer by reannealing in oxygen to produce the 30, 60, and 90 K YBCO phases. A clear shift to lower temperatures of 6–8 K is now observed in the peak position of the ferromagnetic ordering temperature T_p, in the bilayers of the 30 and 60 K YBCO phases, relative to the T_p values of two reference SRO films with high and low resistances. We verified by atomic force microscopy that the different resistances of the two 5 nm thick SRO films are related to morphology changes in the films. This can be due to a slight difference in the miscut angle of the (100) $SrTiO_3$ wafers or to small film thickness variations in different deposition runs. To minimize this large variability in the properties of the SRO films, we prepared additional samples with the reference SRO film on half the area of the wafer and the bilayer on the other half as described in the experimental part above. This geometry is depicted in the inset of Fig. 7. The results of the normalized dR/dT in such a sample are shown in Fig. 7. Basically, the results of Fig. 6 are now reproduced in Fig. 7 in a bilayer with the 60 K YBCO phase where again, a large 6 K shift of T_p is found. This time, however, the results were obtained with two SRO films (one in the bilayer and the other of the reference film) which were prepared in the same deposition run and on the same wafer. Therefore, the variability in the

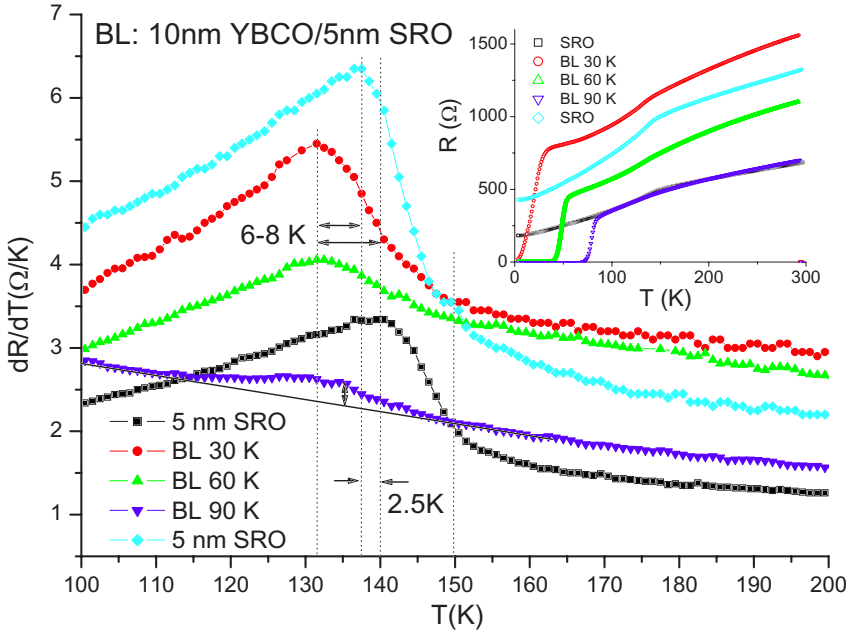

FIG. 6. (Color online) dR/dT versus temperature of the same 10 nm YBCO/5 nm SRO bilayer reannealed to produce the 30, 60, and 90 K YBCO phases, together with the dR/dT data of two 5 nm thick SRO films of high and low resistances. The inset shows the corresponding raw data of R versus T.

SRO properties in this case is minimal, and the reliability and reproducibility of the T_p shift are well established. A smaller shift of T_p of 2–5 K is found in the 90 K bilayer of Fig. 6, but the corresponding dR/dT peak is too small and broad for a clear determination of the shift. Suppression in the magnitude of dR/dT near the SRO peak is evident in all bilayers in Figs. 6 and 7, and more so in the 90 K bilayer, similar to the results of Fig. 4.

Since the largest shifts of the ferromagnetic ordering temperature T_p are observed in the 30 and 60 K bilayers, it is tempting to attribute this behavior to the fact that around 140 K, YBCO with T_c of 30 or 60 K is within its pseudogap regime, while the 90 K phase of YBCO is above its T^*. One possible interpretation is that this phenomenon originates in a proximity effect where preformed pairs with zero spin are injected from the YBCO layer into the adjacent SRO layer and lower its T_p. To investigate this scenario, we performed several control experiments, in which we compared the proximity effect between SRO and different types of conductors, as follows: (i) bilayers of 5 nm SRO with 10 nm thick cuprate films for which the relevant temperature range is not in the pseudogap regime (these include LSCO[16] with $T^* < 100$ K and the 90 K YBCO phase for which the pseudogap regime, if at all, exists only very close to T_c); (ii) bilayers of 5 nm SRO with 10 nm of a normal metal (Au); and (iii) bilayers of 5 nm SRO with 10 nm of an antiferromagnetic metal (Cr). In cases (i) and (ii), single uncorrelated charge carriers are injected into the SRO, while in case (iii), there is a competition between two different types of magnetic order parameters. The proximity effect with an underdoped YBCO should give similar results to case (iii), unless preformed pairs exist. In the latter case, each injected pair carries two charges with zero spin, which should decrease both the polarization and the ferromagnetic correlations in the SRO layer in a more noticeable way than in the case where the injected charges are uncorrelated. One can argue qualitatively that if the underdoped YBCO contains singlet Cooper pairs, the probability of injecting two charges with zero spin into the SRO is $P_{\uparrow\downarrow}=1$ because of the electron-electron correlations, while for uncorrelated electrons, the injection probability $P_{\uparrow\downarrow}$ would be only $P_{\uparrow}P_{\downarrow}=0.5\times0.5=0.25$. Thus, clearly, the injection of correlated pairs should have a stronger effect on T_p, the midpoint of the ferromagnetic transition.

The dR/dT versus temperature results of the bilayers of the control experiments (of which the LSCO data were obtained in the configuration shown by the inset of Fig. 7) are shown in Figs. 8 and 9. This time, the dR/dT peak of the 90 K YBCO bilayer in Fig. 8 is stronger and allows a clear determination of its peak value T_p. Figure 8 shows that the T_p values of both the LSCO and 90 K YBCO bilayers coincide to within the experimental error with that of the SRO reference film at $T_p \approx 139$ K. Moreover, the T_p value of the Cr bilayer of Fig. 9 shifts by only 2 K to lower temperature relative to the reference SRO film, while in the Au bilayer, a similar T_p shift is observed but to higher temperatures. Thus, these ±2 K T_p shifts are significantly smaller than the 6–8 K shifts observed in the 30 and 60 K bilayers of Figs. 6 and 7.

We attribute the small 2 K downshift of T_p of the Cr bilayer in Fig. 9 to a loss of itinerant spin polarized electrons in the SRO layer caused by an inverse proximity effect,

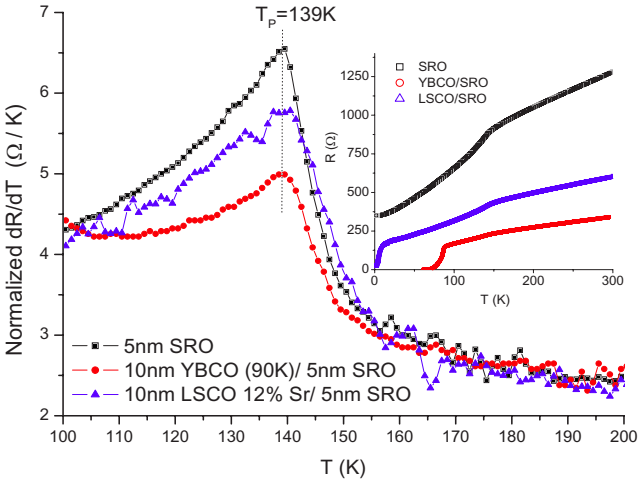

FIG. 8. (Color online) Normalized dR/dT versus temperature of two bilayers, one of a 10 nm YBCO/5 nm SRO of the 90 K YBCO phase and the other of a 10 nm $La_{1.88}Sr_{0.12}CuO_{4-y}$/5 nm SRO, together with the dR/dT data of a 5 nm thick SRO reference film. Normalization to the reference film is done in the 160–180 K temperature range. The inset shows the raw data of R versus T.

where these electrons are injected into the adjacent normal chromium layer. Injection of electrons in the opposite direction into the SRO layer should, in principle, enhance its ferromagnetism due to the presence of the exchange field. This seems to be the case in the Au/SRO bilayer in this figure, where the gold has a higher density of conduction electrons than SRO, but without spin correlations. In the Cr/SRO bilayer, this is not the case since the carriers injected into the SRO, although uncorrelated, may have some degree of antiferromagnetic spin correlations which would tend to hinder the formation of the ferromagnetic order (T_p) in the SRO. Figure 9 shows exactly this for the chromium bilayer, by the small T_p downshift of ~2 K. Thus, injection of uncorrelated electrons with opposite spins does not seem to cause the

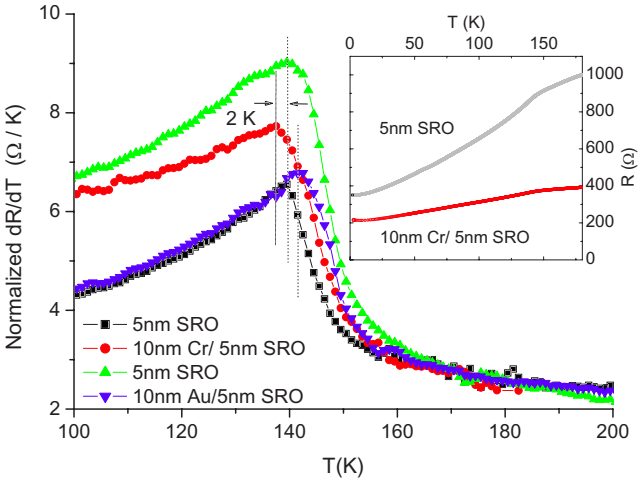

FIG. 9. (Color online) dR/dT versus temperature of 10 nm Cr/5 nm SRO and 10 nm Au/5 nm SRO bilayers normalized to two 5 nm thick SRO reference films. Normalization is done in the 160–180 K temperature range. The inset shows the raw data of R versus T for the Cr bilayer and one of the SRO films.

large downshift of T_p. This leads to the conclusion that the large T_p shifts observed in Figs. 6 and 7 for the 30 and 60 K bilayers are due to injection of correlated electrons, similarly to the preformed pair scenario in the pseudogap regime. One could still argue that the large T_p downshifts are due to the inverse proximity effect, where a loss of itinerant spin polarized electrons occurs as in the chromium case. This, however, would necessitate that the density of states near the Fermi surface of the 90 K YBCO phase be lower than that of the 30 and 60 K phases of YBCO, which is not the case. We note that the density of states in all the hole-doped cuprates, and thus also in YBCO, increases with increasing oxygen doping level. Thus, one can rule out the inverse proximity effect as the responsible mechanism for the large T_p shifts. Our results, therefore, are consistent with the preformed pair scenario but are not a definitive proof for their existence. However, our suggestion that a large effect on T_p is due to the injection of oppositely polarized correlated electrons, from the YBCO layer in the pseudogap regime into the SRO layer, is a significant step in support of the precursor superconductivity scenario in the cuprates.

Finally, we discuss the above conclusion and consider alternative interpretations of our results. First, we wish to discuss possible interdiffusion effects at the interface on our results. From the atomically smooth surface morphology of the SRO layer as seen in Fig. 1, and the various TEM images,[8–10] it is clear that the interface in the bilayers with SRO is sharp and flat. Therefore, interdiffusion in such an interface is quite unlikely. Moreover, even if we assume that reaction products are present at the interface, our results are not affected by them since in the 7.5 nm YBCO/5 nm SRO bilayers (see Fig. 4), no shift of T_p was observed. Thus, the large T_p shifts observed when the YBCO layer was thicker (10 nm thick) have nothing to do with interface reactions, if any, and result from the added amount of YBCO. We also wish to stress that in both Cr/SRO and Au/SRO bilayers, deposition of the Cr and Au layers was done at low temperatures (30 and 150 °C, respectively). Hence, no interdiffusion into the SRO could have occurred in these cases either. Concerning density of states considerations, we note that the similar resistivities of SRO, YBCO, and LSCO indicate that the density of states in these materials is on the same order of magnitude. The density of states of the Cr and Au metals are much higher than that of SRO, and as a result, a higher injection rate into the SRO is expected. This, however, did not lead to larger T_p shifts in these cases. An alternative model for the pseudogap regime involves large superconducting fluctuations above T_c, while phase coherence is reached at T_c. Such a model is consistent with the Nernst results where the onset of this effect follows a higher temperature dome similar to the lower temperature dome at T_c.[17] Our results for the 12% Sr doped LSCO where no T_p shift was observed (Fig. 8) are consistent with the Nernst onset at 110–120 K, since this is out of the ferromagnetic transition range of SRO at 130–150 K. Unfortunately, there are no similar data on the Nernst onset for YBCO, so no further comparison with the YBCO results can be made. We note, however, that our LSCO results are in disagreement with the pseudogap $T^* \approx 160$ K obtained from specific heat measurements[17] but agree well with the $T^* \approx 60$ K obtained from STM results.[16]

In conclusion, using the ferromagnetic transition of SRO as a probe, the YBCO properties in the pseudogap regime were studied in nanometer thick bilayers with SRO. By comparing results of several types of bilayers, we found that the largest effect on the SRO layer occurs when the YBCO is in the pseudogap regime. We conclude that in this regime in YBCO, electrons with opposite spins have to be correlated to produce the much larger effect, and this lends support for the performed pairs scenario.

The authors are grateful to L. Klein and O. Millo for useful discussions and I. Asulin for taking the STM image of Fig. 1. This research was supported in part by the Israel Science Foundation (Grants No. 1564/04 and No. 746/06), the Heinrich Hertz Minerva Center for HTSC, the Karl Stoll Chair in advanced materials, and the Fund for the Promotion of Research at the Technion.

*gkoren@physics.technion.ac.il; URL: http://physics.technion.ac.il/~gkoren

[1] T. Timusk and B. Statt, Rep. Prog. Phys. **62**, 61 (1999).
[2] M. R. Norman, D. Pines, and C. Kallin, Adv. Phys. **54**, 715 (2005).
[3] V. J. Emery and S. A. Kivelson, Nature (London) **374**, 434 (1995).
[4] S. Soltan, J. Albrecht, and H. U. Habermeier, Phys. Rev. B **70**, 144517 (2004).
[5] V. Pena, C. Visani, J. Garcia-Barriocanal, D. Arias, Z. Sefrioul, C. Leon, J. Santamaria, and Carmen A. Almasan, Phys. Rev. B **73**, 104513 (2006).
[6] M. A. Lopez de la Torre, V. Pea, Z. Sefrioui, D. Arias, C. Leon, J. Santamaria, and J. L. Martinez, Phys. Rev. B **73**, 052503 (2006).
[7] Ion C. Moraru, W. P. Pratt, Jr., and Norman O. Birge, Phys. Rev. Lett. **96**, 037004 (2006).
[8] Y. Huang, K. L. Merkle, and K. Char, Microsc. Microanal. **3**, 108 (1997).
[9] H. U. Habermeier and G. Cristiani, Physica C **408-410**, 864 (2004).
[10] T. Holden, H. U. Habermeier, G. Cristiani, A. Golnik, A. Boris, A. Plmenov, J. Humlicek, O. I. Lebedev, G. Van Tendeloo, B. Keimer, and C. Bernhard, Phys. Rev. B **69**, 064505 (2004).
[11] N. Nakagawa, H. Y. Hwang, and D. A. Muller, Nat. Mater. **5**, 204 (2006).
[12] M. E. Fisher and J. S. Langer, Phys. Rev. Lett. **20**, 665 (1968).
[13] S. Alexander, J. S. Helman, and I. Balberg, Phys. Rev. B **13**, 304 (1976).
[14] L. Antognazza, K. Char, T. H. Geballe, L. L. King, and A. W. Sleight, Appl. Phys. Lett. **63**, 1005 (1993).
[15] P. Aronov and G. Koren, Phys. Rev. B **72**, 184515 (2005).
[16] O. Yuli, I. Asulin, G. Koren, and O. Millo, Phys. Rev. B **75**, 184521 (2007).
[17] Y. Wang, L. Li, and N. P. Ong, Phys. Rev. B **73**, 024510 (2006).